Acta Oceanol. Sin., 2019, Vol. 38, No. 3, P. 78–92
https://doi.org/10.1007/s13131-019-1401-y
http://www.hyxb.org.cn
E-mail: hyxbe@263.net

The relative changes of a sea surface temperature in the South China Sea since the Pliocene

Dongjie Bi[1], Daojun Zhang[2], Shikui Zhai[1]*, Xinyu Liu[2], Chun Xiu[1], Xiaofeng Liu[1], Aibin Zhang[1]

[1] Key Laboratory of Submarine Geosciences and Prospecting Techniques of Ministry of Education, College of Marine Geosciences, Ocean University of China, Qingdao 266100, China

[2] Zhanjiang Branch Institute of China National Offshore Oil Corporation (CNOOC) Limited, Zhanjiang 524057, China

Received 15 November 2017; accepted 15 January 2018

Abstract

The reconstruction of sea surface temperature (SST) is a key issue in research on paleoceanography. The recently related studies are mainly concentrated on the Quaternary. The skeletons of a typical species of benthonic foraminifer (*Amphistegina radiata*) in the top 0–375.30 m interval of Well "Xike-1" reef core, Shidao Island, the Xisha Islands, are uniformly selected. The ratios of magnesium to calcium concentrations and other indicators are analyzed by an electron microprobe analysis (EMPA) with the purpose of estimating the paleo-SSTs since the Pliocene and further investigating the periodic change law of paleoclimate in the South China Sea (SCS). Meanwhile, the geologic significance of paleoclimatic events in the SCS is discussed with global perspectives. The results indicate that the paleo-SSTs reconstructed by the ratios of magnesium to calcium concentrations in the SCS show a general periodic trend of "high–low–high–low" in values changes since the Pliocene. By comparison, the fluctuations of reconstructed paleo-SSTs are much stronger in the Quaternary. Moreover, the variations of the ratios of magnesium to calcium concentrations in the *A. radiata* skeletons have recorded a series of major paleoclimatic events since the Pliocene, of which the Quaternary glaciation events and the Arctic ice cap forming events during the late Pliocene are more significant. Thus, using the changes of the ratios of magnesium to calcium concentrations in the *A. radiata* skeletons from Well "Xike-1" reef core to reflect the relative changes of paleo-SSTs is a relatively feasible and reliable way in the SCS, which is also proved by the correlation of drilling cores characteristics in this area.

Key words: the ratios of magnesium to calcium concentrations, benthonic foraminifera, sea surface temperature, paleoclimatic events

Citation: Bi Dongjie, Zhang Daojun, Zhai Shikui, Liu Xinyu, Xiu Chun, Liu Xiaofeng, Zhang Aibin. 2019. The relative changes of a sea surface temperature in the South China Sea since the Pliocene. Acta Oceanologica Sinica, 38(3): 78–92, doi: 10.1007/s13131-019-1401-y

1 Introduction

The reconstruction of paleoceanographic and paleoclimatic records has great significance in exploring the changing laws of global climate and environment. The quantitative reconstruction of the sea surface temperature (SST) is not only the first issue needed to be solved, but also the key to studying the climatic evolution in the earth surface system (Li, 2005). The SST is one of the most important oceanic environment parameters. Reconstructing the SST has become a key issue in research on paleoceanography (Wei et al., 1999). According to the available information, the skeletons are still the most valuable record among all the geological records of the SST. From the methods of paleontological index species and faunal transfer functions to the geochemical methods of stable isotopes and the ratios of magnesium to calcium concentrations (c(Mg)/c(Ca) ratios), and so on, the reconstruction of the SST experiences a process from qualitative, semi-quantitative to quantitative (Guo, 2013). c(Mg)/c(Ca) ratios in foraminiferal skeletons show strong temperature sensitivity due to the temperature-dependent partitioning of magnesium during the calcification process, as a result, the higher the ambient sea water temperature, the more the magnesium being incorporated into carbonate (Nürnberg, 1995; Nürnberg et al., 1996; Lea et al., 1999; Hasenfratz et al., 2017). During the past 2 decades, foraminiferal c(Mg)/c(Ca) thermometry has been successfully used to reconstruct sea water temperatures in the surface and deep ocean (e.g., Lea et al., 2000; Barker et al., 2009; Elderfield et al., 2012). The c(Mg)/c(Ca) ratios in foraminiferal skeletons have been constructed as a good thermometer of the SST.

Recent studies have confirmed that the geochemical characteristics of trace elements in biogenic carbonate can provide important information for the reconstruction of paleoclimate and paleoenvironment (Wei et al., 1999, 2000). Magnesium, strontium, and other elements are incorporated into the skeletons of foraminifera, ostracoda, gastropods, and other aquatic organisms from the sea water directly (Li et al., 2008). Thus, the geochemical characteristics of the trace elements in the skeletons recorded the information about the conditions of surrounding sea water at that time, if never or less influenced by a post-diagenetic alteration. As early as the 1920s, scientists found that there was a cer-

Foundation item: The National Science and Technology Major Project of China under contract No. 2011ZX05025-002-03; the Project of China National Offshore Oil Corporation (CNOOC) Limited under contract No. CCL2013ZJFNO729; the National Natural Science Foundation of China under contract No. 41530963.
*Corresponding author, E-mail: zhai2000@ouc.edu.cn

tain correlation between the magnesium concentrations of skeletons and the SST. From then on, scientists carried out large numbers of experimental works. In the 1990s, they concluded that temperature is the leading mechanism controlling the *c*(Mg)/*c*(Ca) ratio under natural conditions. (Russell et al., 1994; Nürnberg, 1995; Nürnberg et al., 1996; Rosenthal et al., 1997). Since then, the *c*(Mg)/*c*(Ca) ratios and *c*(Sr)/*c*(Ca) ratios (the ratios of strontium to calcium concentrations) in foraminiferal skeletons have been widely considered as potential proxies of the paleo-SST. The electron microprobe analysis (EMPA) technology and other geochemical microanalysis technologies have been quickly developing. The EMPA is extremely useful technologies suitable for elemental analysis of sample compositions and the direct observation of material microstructures. Thus, the reconstruction of the paleo-SST by foraminiferal *c*(Mg)/*c*(Ca) thermometry in the long-time scales becomes possible.

The South China Sea (SCS) is the largest marginal sea of the western Pacific Ocean, which exists in a semi-enclosed environment. It is connected to the East China Sea by the Taiwan Strait and connects to the Pacific Ocean through the Luzon Strait, which is located in the southern region of the South China continent. The uplift of the Qinghai-Tibet Plateau and the formation of the SCS basin are produced by tectonic movements in almost the same geological period (Wang et al., 2015b). A special geographical location and a rapid depositional feature (Sarnthein et al., 1994) amplify the responses to the global climate changes in the SCS (Zhao and Wang, 1999). The SCS, which partly involves the western Pacific warm pool, plays an important role in controlling the East Asian monsoon climate (Wang et al., 1999; Tamburini et al., 2003; Xie et al., 2007; Liu et al., 2010; Zhao et al., 2011). In recent years, the reconstructions of the paleo-SSTs in the SCS were mainly based on the study of coralline (reefs). The reconstruction of long time scale paleo-SSTs was limited by the samples. In this paper, a species of typical benthonic foraminiferal (*Amphistegina radiata*) skeletons in the top 0–375.30 m interval of Well "Xike-1" reef core, Shidao Island, the Xisha Islands, were selected uniformly. The *c*(Mg)/*c*(Ca) ratios and other indicators were analyzed by the EMPA with the purpose of estimating the paleo-SSTs by foraminiferal *c*(Mg)/*c*(Ca) thermometry and further investigating the periodic change law of paleoclimate since the Pliocene in the SCS. Meanwhile, the geologic significance of paleoclimatic events in the SCS was discussed with global perspectives.

2 Samples and analytical methods

Strontium, calcium and magnesium have relatively long residence time of 2.5, 5.1, and 12.0 Ma in the modern ocean (Goldberg and Arrhenius, 1958; Swart, 1981; Vollstaedt et al., 2014). The *c*(Mg)/*c*(Ca) ratios and *c*(Sr)/*c*(Ca) ratios have good stability both in time and space (Veizer, 1989; Wei et al., 2000; Marshall and McCulloch, 2002). During the growth process of foraminifera, the strontium, calcium, magnesium and other elements are incorporated into the foraminiferal skeletons from sea water directly. It has been proved that the paleo-SST is the leading mechanism controlling the *c*(Sr)/*c*(Ca) and *c*(Mg)/*c*(Ca) ratios in the foraminiferal skeletons (Rosenthal et al., 1997). The process of Mg^{2+} substituting Ca^{2+} in the marine carbonate is endothermic. The higher the ambient sea water temperature, the more the magnesium being incorporated into the carbonate (He et al., 1985; Nürnberg, 1995; Nürnberg et al., 1996; Lea et al., 1999). Since the 1990s, some scientists have calculated the empirical relationship between the *c*(Mg)/*c*(Ca) ratios and the ambient sea water temperature: $c(\mathrm{Mg})/c(\mathrm{Ca})\ (\mathrm{mmol/mol})=b\cdot e^{mT}$ (Fig. 1),

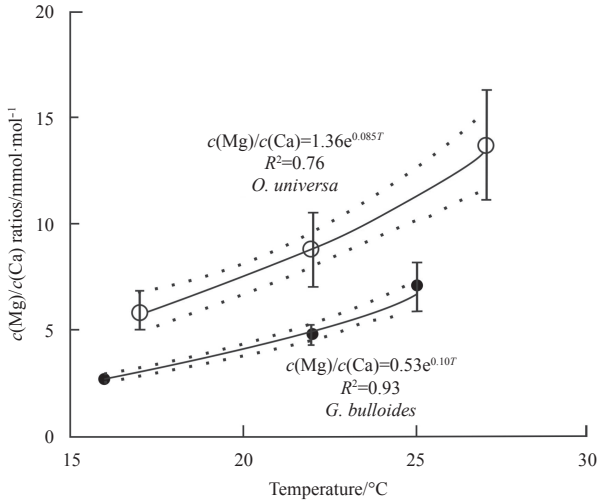

Fig. 1. The plot of *c*(Mg)/*c*(Ca) ratios vs. temperature. The plot was modified from Nürnberg (1995), Nürnberg et al. (1996), Lea et al. (1999), Lea (2003), and Li (2005). The plot indicated the relationship between *c*(Mg)/*c*(Ca) ratios in the foraminiferal skeletons and SST.

where T is the sea water temperature, m and b are constants (Nürnberg, 1995; Nürnberg et al., 1996; Lea et al., 1999; Lea, 2003). Li (2005) indicated that the constant m is between 0.085 and 0.110, the coefficient b is between 0.30 and 0.52 for some foraminiferal species.

The samples selected for this study are from the reef core of Well "Xike-1" located on Shidao Island of Xuande Atoll, the Xisha Islands (16°50′45″N, 112°20′50″E) (Fig. 2). The designated drilling depth of Well "Xike-1" is 1 300.00 m, with complete core recovery and basement drilling. The total length of the drilling core is 1 268.02 m, and the average rate of the core recovery is approximately 80%. Thus far, this site represents the deepest scientific drilling site, with the highest rate of core recovery, in the Xisha area. The complete drilling core with high rate of core recovery provides the basic conditions for reconstructing the paleo-SSTs in the SCS. Despite there are large numbers of coral and foraminiferal fossils in the SCS which can be used as valuable archives for paleoclimate reconstruction, most of them are lack of continuity. Only the skeletons of *A. radiata* are distributed continuously and well preserved (Zhang et al., 2015). According to the sample observation (including microscopic observation), it is found that in an interval below 375.30 m, the drilling core was strongly influenced by a diagenetic alteration and the foraminiferal skeletons were difficult to recognize. Only in an interval above 375.30 m, the skeletons were complete. Thus, depending on the distribution of lithostratigraphic boundaries and complete skeletons, 154 samples were selected from the top 0–375.30 m interval of Well "Xike-1" reef core. The sampling interval ranged from 1.00 to 20.00 m. The average time interval was about 34 ka.

For different species, the parameters taken in the empirical formula purposed by Nürnberg (1995) and Nürnberg et al. (1996) are different (Fig. 1). So far, no empirical formula dependent on the species of *A. radiata* can be referenced in this area. In this article, b=0.52 and m=0.11, were taken by contrast, which were more reasonable and reliable. In addition, the samples experienced different degrees of the diagenetic alteration. Therefore, the paleo-SSTs calculated by the *c*(Mg)/*c*(Ca) ratios in the *A. radiata* skeletons do not represent the true SST values and are just

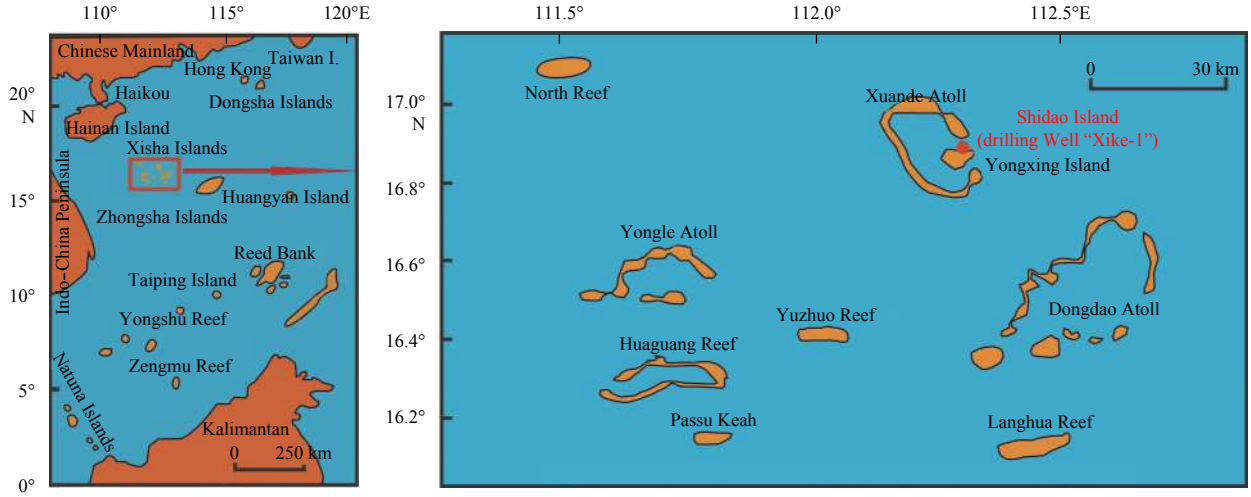

Fig. 2. Simplified map of the Xisha Islands. The Well "Xike-1" is located on Shidao Island of Xuande Atoll, the Xisha Islands.

used to discuss the relative changes of the SST in the SCS since the Pliocene.

In the process of analysis, the skeletons of the same benthonic foraminiferal species (*A. radiata*) were selected (Fig. 3). The analyses were under the same test conditions. The calculation of the paleo-SSTs uniformly selected the same parameter (m=0.11, b=0.52). All these were designed to make sure that the relative changes of the SST reconstructed by the c(Mg)/c(Ca) ratios in the foraminiferal skeletons were reliable.

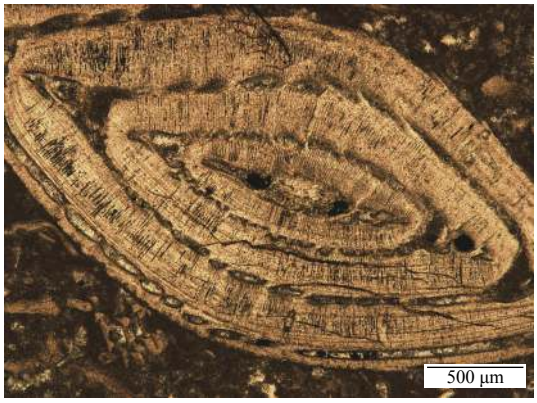

Fig. 3. Photomicrograph of the *A. radiata* skeleton.

2.1 *Sample preparation*

Over 300 samples were selected from the Well "Xike-1" reef core, Shidao Island, the Xisha Islands. The sampling interval was about 2.00 m. Desalinizing the samples as followed: (1) an appropriate amount of sample was immersed in deionized water for 6–8 h; (2) stirred with glass rod to filter out the supernatant; (3) repeated (1) and (2) over three times and placed the samples in an oven at 100°C for 24 h; (4) placed the dried samples in a sealed bag and put them into the clean plastic bottles. The beakers, glass rods, plastic bottles, and so on, used during the treatment were rinsed three times with deionized water. The EMPA sections were made with the desalinized samples.

2.2 *Microscopic observation*

Before the EMPA analysis, the sections with complete (less influenced by the diagenetic alteration) and larger *A. radiata* skeletons (Fig. 3, 154 in total) were selected under an optical microscope.

2.3 *EMPA analysis*

First, the above-mentioned 154 pieces of sections were carbon-coated. Afterwards, the concentrations of strontium, magnesium, calcium, and some other elements (such as iron and manganese) in the skeletons were tested by a JXA-8230 (JEOL) micro-area X-ray spectrometer. The test conditions are as following: the test voltage is 15 kV, the test current is 2.0×10^{-8} A, the beam spot diameter is <1 μm, the test environment temperature is 22°C, the humidity is 40%, and the correction samples are calcium-calcite, magnesium-diopside, strontium-celestite, iron-almandite and manganese-rhodonite. Three or more (3–13) representative points of each skeleton were chosen to analyze based on the results of an EMPA linear analysis (Fig. 4). The average values were shown in Tables 1 and 2.

3 Results

As mentioned above, 154 samples were selected from Well "Xike-1" reef core. The concentrations of strontium, magnesium, calcium, and other elements (e.g., iron and manganese) in a typical species of foraminiferal (*A. radiata*) skeletons were tested by the EMPA technique. The mean c(Mg)/c(Ca) ratios and the relative standard deviation (RSD) values of the c(Mg)/c(Ca) ratios in each sample were also calculated (Table 1). According to the basic principles of statistics, the highly discrete points cannot reflect the true information of the samples. Thus, the highly discrete points (RSD>50%) were left out in the follow discussion. The measured concentrations of magnesium, strontium, calcium, iron, and manganese in the skeletons of *A. radiata* range from 0.1% to 2.7%, 0 to 0.7%, 34.5% to 44.3%, 0 to 0.035%, and 0 to 0.029%, respectively. Whereas the average concentrations of magnesium, calcium, iron, and manganese are 0.5%, 39.6%, 0.009% and 0.009%, respectively (Tables 1 and 2).

As shown in Table 1, the computed c(Mg)/c(Ca) ratios in the skeletons of *A. radiata* range from 3.2 to 116.4 mmol/mol, with a mean value of 21.9 mmol/mol. Whereas the computed c(Sr)/c(Ca) ratios range from 0 to 7.8 mmol/mol. The RSD values of the c(Mg)/c(Ca) ratios in each sample range from 2% to 50%, with a mean value of 23%. The paleo-SSTs reconstructed by c(Mg)/c(Ca) thermometry range from 16.5 to 49.2°C, with a mean value

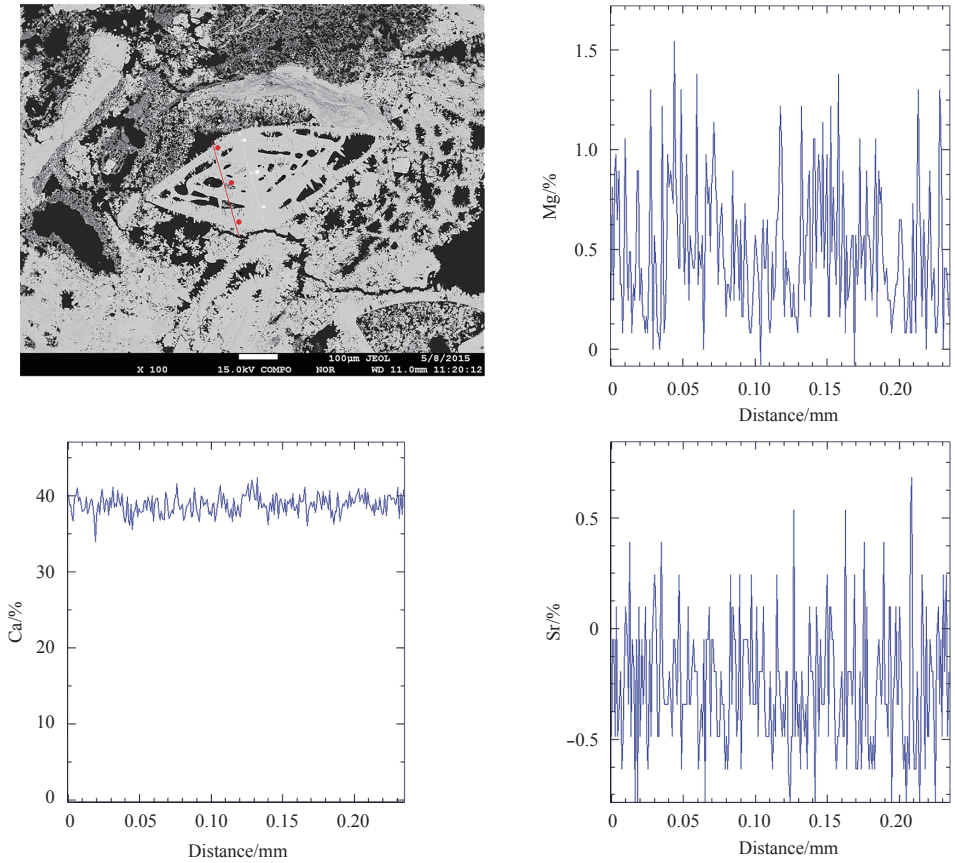

Fig. 4. Secondary electron image of the *A. radiata* skeleton and the results of an EMPA linear analysis. The red dots are the detecting points. The red line is the line of the EMPA linear analysis.

of 32.1°C. The range of paleo-SSTs reconstructed by the *c*(Mg)/*c*(Ca) thermometry is larger than that reconstructed by other indicators, most of the reconstructed paleo-SSTs in this article are higher. Therefore, the reconstructed paleo-SSTs in this article cannot represent the true SST values, which are just used for discussing the relative changes of the SST in the SCS. The reconstructed paleo-SSTs were standardized using 35.9°C (a reconstructed paleo-SST value with the sampling depth of 14.43 m) as a standard in order to indicate the relative changes of the SST better. The standardized paleo-SSTs range from 0.46 to 1.37, with a mean value of 0.89 (Table 1).

4 Discussion

4.1 *Influence of diagenetic alteration*

The element compositions in the skeletons might be influenced by the diagenetic alteration. Because of this, evaluating the effects of diagenesis on the element compositions are very important. The drilled reef sediments generally suffer from two stages of diagenesis: transformation from aragonite to calcite (calcitization) and further into dolomite (dolomitization). It was found that the diagenesis types of the reef carbonates in Well "Xike-1" reef core predominately included weak compaction, neomorphism, micritization, dissolution and cementation during the Quaternary (Zhao et al., 2015). Aragonite and calcite are the major mineral components of the carbonate sediments in the Quaternary (Fig. 5a). Hence, the diagenetic alteration is mainly stay in the superficial phase (calcitization) during this period. Although magnesium-calcite lost Mg^{2+} during the diagenetic period, they may still have sufficient reserves to indicate that the original Mg^{2+} was high (Marshall and Ashton, 1980; Prezbindowski, 1985). Thus, the variations of measured *c*(Mg)/*c*(Ca) ratios can represent the relative changes of the SST during the Quaternary.

In addition, the concentrations of iron and maganese are good indicators for diagenetic alteration of carbonates. The iron and maganese concentrations in the foraminiferal skeletons are very low (<0.04%), which shows no obvious correlation with the mineral compositions of the reef carbonates in Well "Xike-1" reef core (Fig. 5b). As shown in Figs 5a and b, the changes of the mineral compositions in the reef carbonates have no linear dependence relation with that of the *c*(Mg)/*c*(Ca) ratios in the foraminiferal skeletons. The *c*(Mg)/*c*(Ca) ratios do not increase with the concentrations of dolomite. On the contrary, the dolomite layer (289.30–312.30 m) corresponds to the relative low *c*(Mg)/*c*(Ca) ratios. Hence, the diagenetic alteration did not significantly influence the measured *c*(Mg)/*c*(Ca) ratios in the foraminiferal skeletons since the Pliocene. Thus, although the carbonates in Well "Xike-1" reef core experienced different degrees of the diagenetic alteration, the diagenetic alteration did not significantly influence the relative changes of the measured *c*(Mg)/*c*(Ca) ratios in the *A. radiata* skeletons from Well "Xike-1" reef core. The variations of measured *c*(Mg)/*c*(Ca) ratios can represent the relative changes of the SST since the Pliocene in the SCS.

The formation of reefs is harsh for environmental conditions. The SST is one of the important factors controlling the growth of reef-building organisms. Studies have shown that the suitable temperature for corals is 18–30°C (Wang, 2001). The SST ranged

Table 1. Mean concentrations of strontium, magnesium, calcium and the mean values of *c*(Mg)/*c*(Ca), *c*(Sr)/*c*(Ca) ratios in the *A. radiata* skeletons from Well "Xike-1" reef core.

Depth/m	*c*(Mg) (mean)/%	*c*(Sr) (mean)/%	*c*(Ca) (mean)/%	*c*(Mg)/*c*(Ca) (mean)/ mmol·mol^{-1}	RSD /%	*c*(Sr)/*c*(Ca) (mean)/ mmol·mol^{-1}	Paleo-SSTs/°C	Standardized paleo-SSTs
14.43	0.6	–	38.2	27.1	37	–	35.9	1.00
14.73	2.4	0.1	34.5	116.4	41	1.6	49.2	1.37
15.21	0.8	0.1	40.3	31.4	30	1.5	37.3	1.04
15.51	1.0	0.1	38.3	44.3	47	1.3	40.4	1.13
15.81	0.4	–	38.9	17.8	11	–	32.1	0.89
16.26	0.8	0.2	36.2	39.5	107	2.6	39.4	1.10
16.53	0.6	0.1	38.0	27.3	41	1.7	36.0	1.00
16.93	0.9	0.1	39.2	36.8	62	1.5	38.7	1.08
17.32	0.5	–	37.6	20.9	50	–	33.6	0.94
17.62	0.5	0.1	38.9	22.1	35	1.0	34.1	0.95
17.92	1.1	–	38.2	49.9	55	–	41.5	1.16
18.22	0.6	0.2	38.2	25.3	68	1.7	35.3	0.98
18.52	0.6	–	37.6	24.4	14	–	35.0	0.97
19.11	1.0	0.1	39.3	42.0	41	1.2	39.9	1.11
19.41	0.7	0.1	39.8	27.0	4	1.6	35.9	1.00
19.71	1.7	0.1	37.9	75.0	92	1.1	45.2	1.26
20.01	1.6	–	35.4	78.2	110	–	45.6	1.27
20.31	0.8	0.1	41.9	33.7	58	0.9	37.9	1.06
21.06	0.8	–	35.3	38.1	37	–	39.0	1.09
21.36	0.4	–	39.3	17.3	61	–	31.9	0.89
21.66	0.9	0.1	37.2	39.3	29	1.7	39.3	1.09
21.78	0.6	0.1	38.5	24.1	25	1.5	34.9	0.97
22.30	0.4	0.1	38.9	17.6	21	1.4	32.0	0.89
22.60	0.4	0.1	39.3	17.5	58	0.6	32.0	0.89
24.15	0.5	–	36.0	22.7	63	–	34.3	0.96
24.91	0.5	0.1	39.4	20.0	8	1.3	33.2	0.92
25.21	0.5	0.1	35.9	21.5	50	0.9	33.8	0.94
25.98	0.6	0.1	39.9	23.2	23	1.3	34.5	0.96
26.78	0.6	–	40.0	24.5	69	–	35.0	0.97
27.08	0.2	0.1	38.2	9.9	41	0.5	26.8	0.75
27.54	0.4	0.4	41.4	14.3	76	3.9	30.1	0.84
28.14	0.5	0.1	39.3	21.0	49	1.0	33.6	0.94
28.44	0.1	–	39.8	3.2	32	–	16.5	0.46
29.31	0.1	0.1	38.7	6.0	34	1.6	22.3	0.62
29.61	0.1	0.7	42.0	3.5	12	7.8	17.4	0.48
30.49	0.2	0.1	39.9	7.5	28	1.5	24.3	0.68
31.35	0.1	0.1	39.5	5.1	11	0.6	20.7	0.58
32.12	0.3	0.2	36.5	14.0	41	2.0	30.0	0.84
32.68	0.4	0.3	39.6	15.0	106	3.2	30.5	0.85
33.29	0.3	0.1	40.8	11.6	23	1.2	28.2	0.79
34.58	0.7	0.3	36.8	33.4	76	3.7	37.8	1.05
35.48	0.6	–	36.9	28.0	76	–	36.2	1.01
36.13	0.6	0.1	39.0	24.9	11	1.2	35.2	0.98
36.69	0.4	0.1	39.4	16.9	6	1.1	31.6	0.88
37.29	0.4	0.0	38.7	18.8	5	0.5	32.6	0.91
38.14	2.7	0.1	39.8	113.9	17	0.5	49.0	1.36
39.31	0.4	0.1	38.7	14.9	14	1.6	30.5	0.85
39.97	0.4	–	38.8	16.1	14	–	31.2	0.87
40.24	0.3	0.2	38.9	13.4	26	2.8	29.5	0.82
42.00	0.2	0.1	39.2	8.7	41	1.3	25.6	0.71
42.55	0.1	0.0	40.2	4.8	16	0.3	20.1	0.56
43.15	0.2	0.1	39.7	6.2	23	1.2	22.5	0.63
44.05	0.3	0.2	38.5	11.6	8	2.8	28.2	0.79
44.35	0.2	0.2	39.7	6.4	14	2.6	22.9	0.64
44.87	0.2	0.1	36.9	8.4	74	0.6	25.3	0.70

to be continued

Continued from Table 1

Depth/m	*c*(Mg) (mean)/%	*c*(Sr) (mean)/%	*c*(Ca) (mean)/%	*c*(Mg)/*c*(Ca) (mean)/ mmol·mol^{-1}	RSD /%	*c*(Sr)/*c*(Ca) (mean)/ mmol·mol^{-1}	Paleo-SSTs/°C	Standardized paleo-SSTs
45.17	0.1	0.2	39.5	6.0	30	2.5	22.2	0.62
45.47	0.2	0.2	39.3	6.5	29	1.9	22.9	0.64
46.34	0.1	0.0	40.1	6.0	73	0.4	22.2	0.62
46.63	0.1	0.1	39.2	6.1	52	1.2	22.3	0.62
47.26	0.1	0.1	39.6	6.0	55	1.3	22.2	0.62
48.12	0.4	0.2	39.7	15.2	28	2.0	30.7	0.86
48.54	0.2	0.2	39.9	7.8	42	1.8	24.6	0.69
49.19	0.3	0.2	39.2	13.7	40	1.7	29.7	0.83
50.07	0.4	0.2	38.1	18.6	41	2.2	32.5	0.91
50.37	0.3	0.1	37.7	10.9	36	1.0	27.6	0.77
51.00	0.4	0.2	38.9	14.8	8	1.7	30.4	0.85
51.67	0.4	0.2	37.6	15.4	8	1.9	30.8	0.86
52.49	0.4	0.1	40.4	16.9	83	1.1	31.6	0.88
53.11	0.4	0.2	39.2	14.9	74	2.0	30.5	0.85
54.32	0.2	0.2	38.3	7.3	15	1.8	24.0	0.67
54.62	1.4	0.1	40.9	56.2	22	0.9	42.6	1.19
55.44	0.2	0.1	38.4	9.4	26	1.5	26.3	0.73
56.12	0.3	–	39.3	13.1	25	–	29.4	0.82
57.17	0.1	0.2	39.7	6.1	9	2.3	22.3	0.62
59.21	0.4	0.2	39.3	16.9	27	2.3	31.7	0.88
59.51	0.1	0.0	39.3	3.0	50	0.5	15.9	0.44
60.10	0.7	0.5	38.0	32.5	9	5.6	37.6	1.05
60.97	0.5	0.1	40.2	20.6	4	1.5	33.5	0.93
61.29	0.2	0.2	39.0	6.3	46	2.7	22.6	0.63
62.49	0.4	0.2	40.4	15.5	20	1.8	30.8	0.86
63.30	0.4	0.2	40.7	15.0	2	2.5	30.5	0.85
65.30	0.3	0.1	41.0	13.8	21	1.6	29.8	0.83
71.32	0.5	0.1	42.2	18.2	29	1.4	32.3	0.90
73.30	0.4	0.1	39.0	17.0	13	1.3	31.7	0.88
76.98	0.4	0.1	40.3	14.7	15	1.0	30.4	0.85
80.30	0.3	0.1	36.6	15.0	15	0.8	30.6	0.85
84.38	0.3	0.1	40.2	11.9	36	0.9	28.5	0.79
106.30	0.1	0.1	38.8	5.6	67	1.0	21.5	0.60
110.30	0.2	0.0	42.8	5.8	25	0.2	22.0	0.61
118.30	0.2	0.1	42.3	6.6	85	1.2	23.1	0.64
120.30	0.2	0.1	41.9	7.2	14	0.8	23.8	0.66
128.30	0.2	0.0	44.1	6.4	30	0.5	22.8	0.64
143.00	0.2	0.0	41.8	7.9	23	0.5	24.7	0.69
147.30	0.2	0.0	42.1	6.5	20	0.2	22.9	0.64
148.60	0.2	0.0	41.8	6.5	26	0.5	23.0	0.64
149.30	0.3	0.1	44.2	9.7	11	0.6	26.6	0.74
153.30	0.3	0.1	42.3	11.3	44	1.0	28.0	0.78
156.30	0.2	0.1	41.8	9.8	7	1.1	26.7	0.74
173.27	0.4	0.1	40.5	16.0	47	1.4	31.1	0.87
178.30	0.5	0.1	40.8	20.1	10	1.0	33.2	0.92
186.30	0.6	0.1	42.5	23.9	23	1.4	34.8	0.97
188.30	0.6	0.1	34.8	26.7	13	1.7	35.8	1.00
190.30	0.8	0.1	39.5	33.8	32	1.3	38.0	1.06
192.30	1.0	0.1	41.8	38.6	10	0.6	39.2	1.09
202.15	0.7	0.1	40.2	27.2	13	1.1	36.0	1.00
211.20	0.8	0.2	42.0	32.8	17	1.7	37.7	1.05
213.30	0.6	0.1	35.8	27.5	29	1.0	36.1	1.01
215.30	0.8	0.2	42.4	32.9	32	1.8	37.7	1.05
219.30	0.9	0.1	40.5	38.6	22	1.3	39.2	1.09

to be continued

Continued from Table 1

Depth/m	*c*(Mg) (mean)/%	*c*(Sr) (mean)/%	*c*(Ca) (mean)/%	*c*(Mg)/*c*(Ca) (mean)/ mmol·mol^{-1}	RSD /%	*c*(Sr)/*c*(Ca) (mean)/ mmol·mol^{-1}	Paleo-SSTs/°C	Standardized paleo-SSTs
221.30	1.1	0.1	41.7	44.4	13	0.9	40.4	1.13
223.60	0.7	0.1	42.4	25.5	47	1.6	35.4	0.99
228.90	0.9	0.1	42.5	35.6	26	1.4	38.4	1.07
230.40	0.5	0.1	37.5	22.0	23	0.8	34.0	0.95
232.81	0.7	0.1	40.0	30.2	26	1.5	36.9	1.03
238.30	0.7	0.1	41.2	27.2	55	1.2	36.0	1.00
242.30	0.6	0.1	40.9	24.4	45	1.4	35.0	0.97
245.30	0.8	0.2	42.0	31.6	25	1.6	37.3	1.04
246.30	0.9	0.0	37.2	39.7	23	0.4	39.4	1.10
251.30	0.9	0.2	42.2	33.7	21	1.7	37.9	1.06
255.30	0.6	0.2	41.3	23.5	42	1.8	34.7	0.97
257.30	0.4	0.2	42.6	15.7	24	1.8	31.0	0.86
259.30	0.7	0.0	37.1	32.7	10	0.5	37.7	1.05
261.30	0.5	0.1	41.0	18.3	51	1.3	32.4	0.90
263.30	0.5	0.1	37.2	22.1	19	0.9	34.1	0.95
268.30	0.4	0.1	43.3	15.1	15	1.5	30.6	0.85
270.30	0.6	0.1	35.7	90.5	118	1.0	46.9	1.31
272.30	0.6	0.1	39.7	25.6	21	1.3	35.4	0.99
276.30	0.5	0.1	39.8	20.1	19	1.2	33.2	0.92
278.30	0.5	0.1	37.4	21.0	11	0.7	33.6	0.94
280.30	0.6	0.1	42.2	21.8	22	1.3	34.0	0.95
282.30	0.6	0.1	36.9	25.0	14	1.2	35.2	0.98
285.30	0.6	0.1	41.7	24.9	11	1.0	35.2	0.98
288.30	0.5	0.1	40.7	21.6	7	0.9	33.9	0.94
304.30	0.5	0.1	42.1	21.1	8	1.1	33.6	0.94
309.30	0.5	0.0	42.3	21.2	19	0.5	33.7	0.94
311.30	0.4	0.1	35.5	19.4	9	0.7	32.9	0.92
317.30	0.5	0.1	42.4	18.7	11	1.3	32.5	0.91
320.30	0.5	0.1	40.6	21.2	7	1.2	33.7	0.94
323.30	0.4	0.1	38.2	16.8	21	1.4	31.6	0.88
325.30	1.4	0.1	36.3	65.8	61	1.4	44.0	1.23
327.30	0.9	0.1	36.9	43.3	115	1.1	40.2	1.12
333.30	0.6	0.1	39.3	24.0	25	0.9	34.8	0.97
337.30	0.7	0.1	39.7	28.2	25	1.0	36.3	1.01
342.30	0.6	0.1	41.4	23.4	26	1.0	34.6	0.96
344.30	0.6	0.1	36.2	28.1	28	1.2	36.3	1.01
346.30	0.4	0.1	42.8	16.3	13	1.1	31.3	0.87
348.30	0.6	0.1	37.3	27.3	41	1.5	36.0	1.00
356.30	0.6	0.1	36.2	25.7	25	1.3	35.4	0.99
360.30	0.5	0.1	35.1	23.8	32	1.1	34.8	0.97
362.30	0.5	0.1	39.5	22.0	27	0.9	34.0	0.95
366.30	0.6	0.1	44.3	20.9	14	1.1	33.6	0.94
368.30	1.5	0.1	34.7	73.5	47	0.7	45.0	1.25
370.30	0.4	0.1	39.3	14.8	25	0.9	30.5	0.85
375.30	0.5	0.1	40.1	20.3	10	1.2	33.3	0.93

Note: "–" means below the limit of detection. The paleo-SSTs were calculated by the formula: *c*(Mg)/*c*(Ca) (mmol/mol)=$b \cdot e^{mT}$, b=0.52 and m=0.11. Standardizing the paleo-SSTs reconstructed by the *c*(Mg)/*c*(Ca) thermometry using 35.9°C (a reconstructed paleo-SST with the sampling depth of 14.43 m) as a standard. The relative standard deviation values (RSD) of the *c*(Mg)/*c*(Ca) ratios in each sample were also provided.

from 23.3°C to 28°C during the Holocene and 21.5°C to 25°C during the last glacial period in the northern SCS. The lowest temperature occurred in the marine isotope stage 2 (MIS 2) (Pelejero et al., 1999; Oppo and Sun, 2005; Zhang et al., 2005; Wei et al., 2007; Li et al., 2012). Thus, even during the glacial period, the SST was still suitable for corals and other reef-building organisms, the coral reefs still could develop in the SCS. As mentioned above, the range of paleo-SSTs reconstructed by the *c*(Mg)/*c*(Ca) thermometry is from 16.5°C to 49.2°C, which is larger than that reconstructed by other indicators. The main reason for this may be that reconstructing the paleo-SSTs by the *c*(Mg)/*c*(Ca) ratios in *A. radiata* skeletons has not been studied before. No empirical formula dependent on the species of *A. radiata* could be referenced in the study area. Because of this, the selection of parameters (*b*

Table 2. Mean concentrations of iron and manganese in the *A. radiata* skeletons from Well "Xike-1" reef core

Depth/m	*c*(FeO) (mean)/%	*c*(MnO) (mean)/%	*c*(Fe) (mean)/%	*c*(Mn) (mean)/%
63.30	0.006	0.022	0.005	0.017
65.30	0.001	0.010	0.001	0.008
71.32	0.027	0.018	0.021	0.014
73.30	0.045	0.010	0.035	0.007
76.98	0.011	0.006	0.009	0.005
80.30	0.006	0.010	0.005	0.008
84.38	0.043	0.004	0.033	0.003
106.30	0.016	0.010	0.012	0.008
110.30	0.022	0.022	0.017	0.017
118.30	0.019	0.012	0.015	0.009
120.30	0.021	0.000	0.016	0.000
128.30	0.009	0.003	0.007	0.002
143.00	0.018	0.003	0.014	0.002
147.30	0.000	0.000	0.000	0.000
148.60	0.000	0.031	0.000	0.024
149.30	0.012	0.016	0.010	0.012
153.30	0.003	0.018	0.003	0.014
156.28	0.019	0.000	0.015	0.000
173.27	0.010	0.006	0.008	0.004
178.30	0.005	0.015	0.004	0.011
186.30	0.005	0.019	0.004	0.014
190.30	0.002	0.013	0.001	0.010
192.30	0.025	0.000	0.020	0.000
202.15	0.022	0.006	0.017	0.005
211.20	0.012	0.006	0.009	0.004
215.30	0.002	0.005	0.002	0.004
219.30	0.006	0.038	0.004	0.029
221.30	0.021	0.020	0.016	0.016
223.64	0.003	0.016	0.002	0.013
228.01	0.000	0.007	0.000	0.006
232.81	0.011	0.020	0.008	0.015
238.30	0.007	0.026	0.005	0.020
242.30	0.003	0.006	0.002	0.005
245.30	0.009	0.010	0.007	0.008
251.30	0.014	0.015	0.011	0.012
255.30	0.012	0.024	0.010	0.019
257.30	0.000	0.007	0.000	0.005
261.30	0.008	0.008	0.006	0.006
268.30	0.030	0.004	0.024	0.003
272.30	0.012	0.007	0.009	0.006
276.30	0.003	0.006	0.002	0.005
280.30	0.021	0.009	0.016	0.007
285.30	0.007	0.013	0.006	0.010
288.30	0.006	0.016	0.005	0.013
304.30	0.016	0.004	0.013	0.003
309.30	0.026	0.017	0.020	0.013
317.30	0.023	0.018	0.018	0.014
320.30	0.017	0.012	0.013	0.009
323.30	0.037	0.000	0.029	0.000
327.30	0.009	0.014	0.007	0.011
333.30	0.005	0.010	0.004	0.008
337.30	0.000	0.000	0.000	0.000
342.30	0.010	0.000	0.008	0.000
346.30	0.005	0.008	0.004	0.006
352.30	0.007	0.013	0.006	0.010
362.30	0.011	0.028	0.008	0.022
366.30	0.003	0.020	0.002	0.016
370.30	0.005	0.005	0.004	0.004
375.30	0.013	0.011	0.010	0.008

and *m*) was lack of existing standards. Moreover, although the selected fossils are complete individuals of the same species, the chemical compositions of the fossils may be more or less affected by the diagenetic alteration. Owing to the above-mentioned limitations, the reconstructed paleo-SSTs are not the true SST values at the corresponding time, but they can be used to investigate the relative changes of the SST based on the above discussion. Some paleoclimatic events, especially the drastically fluctuation of the SST under the background of glacial/interglacial alternations during the Quaternary, have good responses on the changes of the *c*(Mg)/*c*(Ca) ratios (Fig. 5b).

4.2 *Characteristics of the reconstructed paleo-SSTs in the SCS*

The paleo-SSTs reconstructed by the *c*(Mg)/*c*(Ca) ratios in the *A. radiata* skeletons from Well "Xike-1" reef core have shown a general periodic trend of "high-low-high-low" periodic cycle in values variations since the Pliocene (Fig. 6). The reconstructed paleo-SSTs fluctuated significantly, especially during the Quaternary, which overall showed a trend of rising. The changing process of the reconstructed paleo-SSTs can be substantially divided into four stages from the bottom to the upper:

The interval of 246.30–375.30 m (about 2.7–5.3 Ma) corresponds to a low temperature period. The standardized paleo-SSTs range from 0.85 to 1.25 in this period, with a mean value of 0.96.

The interval of 190.30–246.30 m (about 1.8–2.7 Ma) corresponds to a high temperature period. The standardized paleo-SSTs range from 0.95 to 1.13 in this period, with a mean value of 1.04. The variations of the reconstructed paleo-SSTs are relatively significant and the climate is instable.

The interval of 63.30–190.30 m (about 0.8–1.8 Ma) corresponds to another low temperature period. The standardized paleo-SSTs range from 0.61 to 1.06, with a mean value of 0.80. During this period, the reconstructed paleo-SSTs are generally low and stable.

The interval of 0–63.30 m (about 0–0.8 Ma) corresponds to the fluctuating period. The maximum and minimum values of the reconstructed paleo-SSTs appear during this period. The standardized paleo-SSTs range from 0.46 to 1.37, with a mean value of 0.86. Significant variations of the reconstructed paleo-SST indicate that the climate changed sharply during the Quaternary, with the main feature of glacial/interglacial alternations.

The sudden change of *c*(Mg)/*c*(Ca) ratios near the depth of 36.00 m indicates an obvious change of the paleoclimate. In the vicinity of the interface, mineral compositions and other parameters of geochemical characteristics also existed a significant change. The causes are still uncertain (Zhai et al., 2015). According to the evidences provided in this article, there should be an important paleoenvironmental changing interface near the depth of 36.00 m.

In addition, the fluctuating period (0–63.30 m) of the reconstructed paleo-SSTs can be further subdivided into four periodic cycles (Fig. 7). The corresponding geological age at the depth of 63.30 m is about 0.8 Ma. The significant variations of the reconstructed paleo-SSTs indicate that the climate was very instable under the background of glacial/interglacial alternations during the Quaternary. The reconstructed paleo-SSTs during this period overall show an upward trend.

4.3 *Changes of the reconstructed paleo-SSTs in the SCS respond to the global paleoclimatic events*

The Quaternary glaciation events were global glacial events, which began from about 2 Ma. The Quaternary glaciation events were the most recent large glaciation events during the geologic-

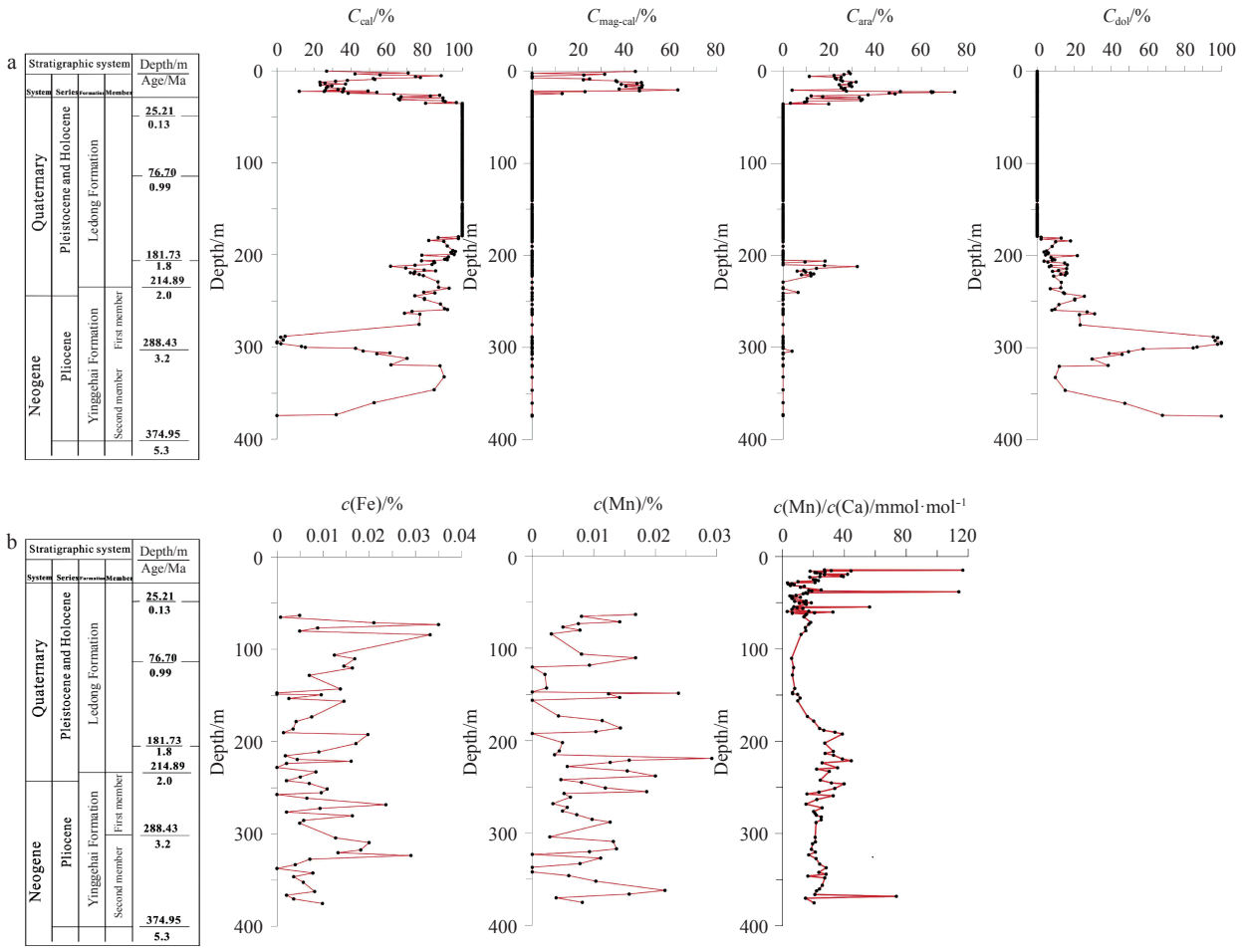

Fig. 5. Plots of the mineral compositions in the reef carbonates of Well "Xike-1" reef core (a) and plots of the iron, manganese concentrations and c(Mg)/c(Ca) ratios in the *A. radiata* skeletons from Well "Xike-1" reef core (b). cal represents calcite, ara aragonite, dol dolomite, and mag-cal magnesium-calcite. The mineral compositions of carbonates were from Zhai et al. (2015), Xiu et al. (2015), and Cao et al. (2016). The data of stratigraphic division and chronological subdivision were from Wang et al. (2015), Zhai et al. (2015), Zhu et al. (2015), Xiu et al. (2015), Zhao et al. (2015), Qiao et al. (2015), You et al. (2015), Ma et al. (2015), and Bi et al. (2017); followed as the same.

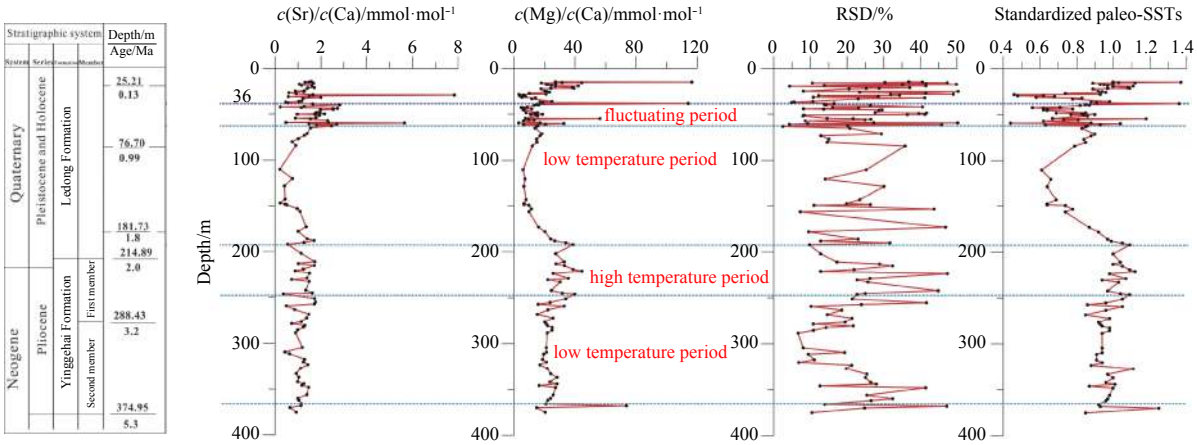

Fig. 6. Plots of the c(Mg)/c(Ca) and c(Sr)/c(Ca) ratios in the *A. radiata* skeletons and the standardized paleo-SSTs. The relative standard deviation (RSD) values of the c(Mg)/c(Ca) ratios in each sample were also provided.

al history. During this period, the climate changed sharply, with the glacier advancing and retreating many times. The global relative sea level also changed many times in this period. The Quaternary glaciation events can be divided into many glacial and in-

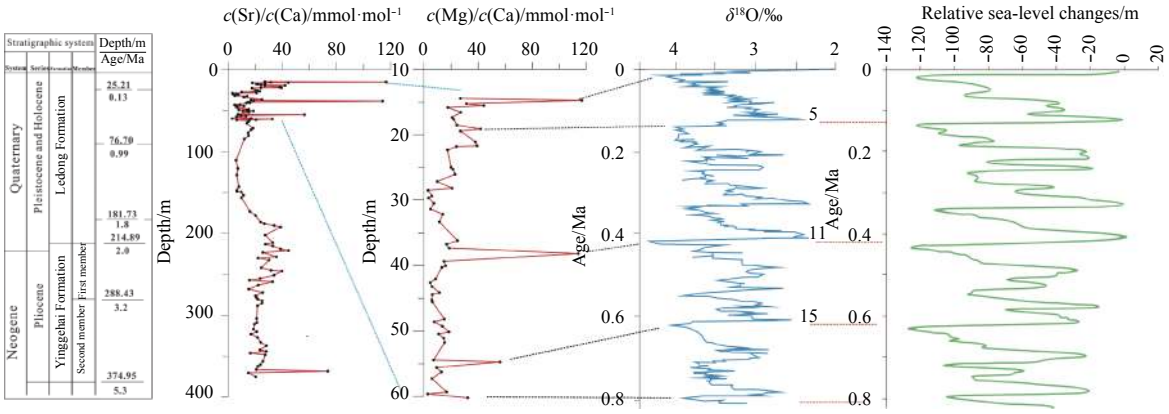

Fig. 7. Plots of the c(Mg)/c(Ca) ratios in the *A. radiata* skeletons, the sea water δ^{18}O values recorded by the benthonic foraminifera, and the relative changes of the global sea level. The sea water δ^{18}O data recorded by the benthonic foraminifera in the drilling core of ODP Site 1148 were derived from Wang et al. (2001). The data of relative sea-level changes was derived from Bintanja et al. (2005). These plots indicate that there is a good correlation among the changes of c(Mg)/c(Ca) ratios, the variations of sea water δ^{18}O values, and the relative changes of the global sea level.

terglacial periods, which were characterized by the glacial/interglacial alternations. The global temperature was further reduced and the Arctic ice cap was further expanded in this period. The glaciers were widely distributed all over the world (Wang et al., 2001; Li et al., 2016).

According to the evidences of moraines, glacial erosion landforms, and sporopollen of cold-tolerant plants all over the world, the Quaternary glaciation events can be roughly divided into four-six sub-glacial periods with sharp changes of the temperature (Yang et al., 1979; Zhao, 1985, 1986). Among them, the four sub-glacial periods of Würm, Riss, Mindel, and Günz, which were classified according to the landforms of moraine and glacial erosion in the Alps area, were popular abroad (Raymo, 1997). However, the four sub-glacial periods of Dali, Poyang, Dagu, and Lushan, which were classified according to the remnants of glacial erosion in the Lushan area and the glacial relics in the western China, were popular in China (Li, 1940; Yang and Xu, 1980; Deng, 1992).

On the basis of mineralogy, geochemistry, and paleontology studies of the reef carbonates from Well "Xike-1" reef core, a series of stratigraphic and chronologic boundaries were identified (Wang, Cui et al., 2015; Zhai et al., 2015; Zhu et al., 2015; Xiu et al., 2015; Zhao et al., 2015; Qiao et al., 2015; You et al., 2015; Ma et al., 2015). Combined with the variation trend and the chronological data, the c(Mg)/c(Ca) ratios in the *A. radiata* skeletons of Well "Xike-1" reef core can be used to compare with other paleoclimatic indicators, although the age control of the Well "Xike-1" reef core is relatively poor. Comparisons among the changes of c(Mg)/c(Ca) ratios in the *A. radiata* skeletons from Well "Xike-1" reef core, the changes of sea water δ^{18}O values recorded by the benthonic foraminifera in the drilling core of ODP Site 1 148, and the relative changes of global sea level (Figs 7, 8 and 9) show that there is a good correlation among the three. The significant fluctuation period of the reconstructed paleo-SSTs coincides with the sharp change period of the global relative sea level. The four periodic cycles of the c(Mg)/c(Ca) ratios in the fluctuating period (0–63.3 m) are consistent with the four significant variations of the sea water δ^{18}O values: MIS 2, 6, 12 and 16. Similar variations of sea water δ^{18}O values were also observed in other sea areas (e.g., ODP 677) (Wang et al., 2001). Moreover, the above-mentioned results also can demonstrate the feasibility of reconstructing the paleo-SSTs by the c(Mg)/c(Ca) ratios in the *A. radiata* skeletons from Well "Xike-1" reef core.

MIS 2, 6, 12 and 16 correspond to the four sub-glaciations in the Alps area, respectively (Figs 7 and 8): MIS 2 corresponds to the Würm glaciation, MIS 6 corresponds to the Riss glaciation, MIS 12 corresponds to the Mindel glaciation, whereas MIS 16 corresponded to the Günz glaciation (Raymo, 1997). Moreover, the Baoji section is judged to be the most complete and accessible Quaternary loess-paleosol section in the north-central China Loess Plateau (Ding and Liu, 1991; Rutter et al, 1990). There is a good corresponding relationship between the changes of sea water δ^{18}O values and the stratigraphy at Baoji (Fig. 8). MIS 2, 6, 12 and 16 corresponded to the thick loess units L_1, L_2, L_5 and L_6, respectively (Ding and Liu, 1991). These thick loess units indicate the glacial climate. These sub-glaciations were characterized by glacier advanced in the mountainous areas and sea level regressed in coastal areas all over the world, which were global phenomenon (Wang et al., 2001). In addition, these four sharp changes in the temperature also had responds in the SCS which was non-glaciation areas. It indicates that the variations of c(Mg)/c(Ca) ratios in the foraminiferal skeletons well recorded the global paleoclimatic events with a sharply temperature fluctuate. Moreover, the c(Mg)/c(Ca) ratios are relatively low in an interval of 63.30–190.30 m, which may represent a large glacial event with a long duration in the geological history. During this period, the paleo-SSTs were relatively low.

In addition, the Arctic ice cap forming events during the Late Pliocene were also global paleoclimatic events in the geological history, which changed the earth from "unipolar ice cap" to "bipolar ice cap". It turned to the glacial climate all over the world during this period. The carbon and oxygen isotopes of the benthonic foraminifera in the SCS (ODP Site 1 148) were significantly heavier in this period (Fig. 9) (Zhao et al., 2001). As shown in Fig. 9, these global paleoclimatic events also have manifestations on the variations of c(Mg)/c(Ca) ratios in the *A. radiata* skeletons from Well "Xike-1" reef core. The c(Mg)/c(Ca) ratios during this period are relatively low (Figs 8 and 9). Moreover, the dolomite layer (289.30~312.30 m) corresponds to the relative low c(Mg)/c(Ca) ratios, which indicates that the dolomite layer was formed during the glacial climate. It is consistent with the research results based on the geochemical researches of reef car-

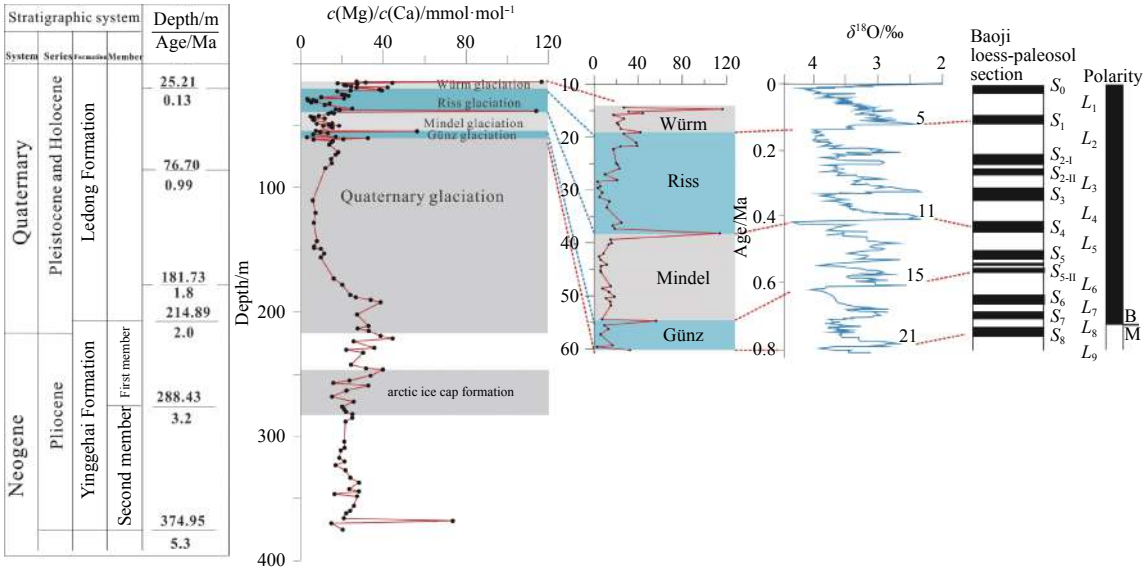

Fig. 8. Correspondence relationship between the variations of c(Mg)/c(Ca) ratios and the global paleoclimatic events. The data of Baoji section were modified from Ding and Liu (1991). The sea water δ^{18}O data recorded by the benthonic foraminifera in the drilling core of ODP Site 1148 were derived from Wang et al. (2001).

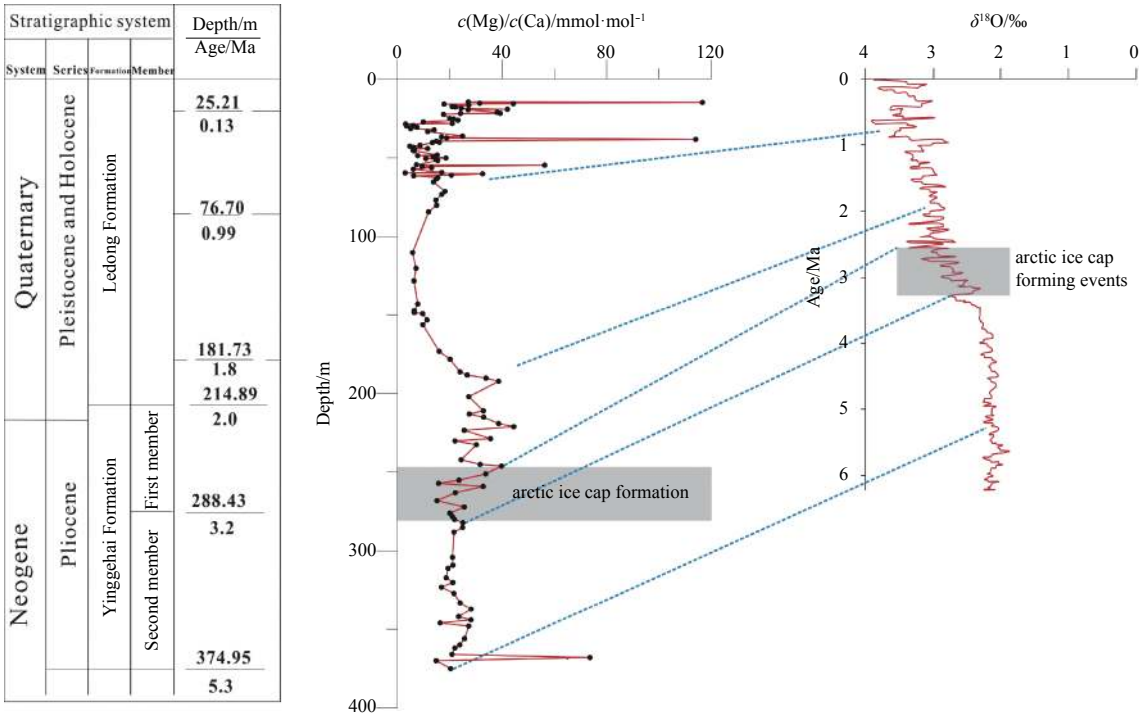

Fig. 9. Correspondence relationship between the variations of c(Mg)/c(Ca) ratios and that of sea water δ^{18}O values. The sea water δ^{18}O values recorded by the benthonic foraminifera in the drilling core of ODP Site 1 148 were derived from Wang et al. (2003).

bonates from Well "Xike-1" reef core (Zhai et al., 2015; Xiu et al., 2015; Cao et al., 2016; Bi et al., 2018).

In summary, the variations of the c(Mg)/c(Ca) ratios in the foraminiferal skeletons from Well "Xike-1" reef core have relative good responses to the major global paleoclimatic events. The fluctuating period of the reconstructed paleo-SSTs in an interval of 0–63.30 m corresponds to the four sub-glaciations of the Quaternary glaciation events. The low temperature period of the reconstructed paleo-SSTs in an interval of 246.30–272.30 m corresponds to the Arctic ice cap forming events during the Late Pliocene.

4.4 *Comparison of the drilling cores characteristics in Xisha area*

The Well "Xiyong-1" is a scientific drilling located on Yongxing Island, the Xisha area. Many scholars have conducted detailed studies on the reef core of Well "Xiyong-1" since the 1970s (Wang et al., 1979; Zhang et al., 1994; Zhao, 2010). The comparison results reveal that there is a positive correlation between the

variations of c(Mg)/c(Ca) ratios in the *A. radiata* skeletons from the top 0–375.30 m interval of Well "Xike-1" reef core and the changes of δ^{18}O values in reef carbonates from the top 0–350.00 m interval of Well "Xiyong-1" (Fig. 10). They both show a general periodic trend of "high-low-high-low" in values variations. As shown in Fig. 10, the rangeability of c(Mg)/c(Ca) ratios are greater than that of the δ^{18}O values, which indicates that the c(Mg)/c(Ca) ratios are more sensitive to the changes of environmental conditions, especially to the changes of the SST. Moreover, it further indicates that the relative changes of the paleo-SSTs in this region were well recorded by the c(Mg)/c(Ca) ratios in the *A. radiata* skeletons. The Well "Xike-1" is the deepest scientific drilling with the highest rate of core recovery in the Xisha area, which has a higher resolution than the Well "Xiyong-1". Therefore, using the c(Mg)/c(Ca) ratios in the *A. radiata* skeletons from Well "Xike-1" reef core to reflect the relative changes of the SST in this area is feasible and reliable.

It should be noted that, according to the mineralogical studies of Well "Xike-1" reef core (Zhai et al., 2015), a thick layer of dolomite is found below 375.30 m. However, in an interval above 375.30 m, the dolomitization is weak and dolomite minerals are not present in most stratus. The dolomitization must have significant impact on the chemical compositions of the reef carbonates, especially on the concentrations of magnesium and calcium. The microscopic observation of the sections find that in an interval below 375.30 m, the *A. radiata* skeletons in the reef core are influenced by the diagenetic alteration and the outline of the skeletons are blurred (Fig. 11). Moreover, the analysis results also show that in an interval below 375.30 m, the concentrations of Mg in the *A. radiata* skeletons are more than 10%, the highest is even about 20%. These indicate that there should be a diagenesis changing interface near the depth of 375.30 m and the c(Mg)/c(Ca) ratios in the *A. radiata* skeletons from Well "Xike-1" reef core below 375.30 m cannot be used to reflect the paleoceanographic characteristics of the sea water in the SCS during the geological history. Therefore, only the samples selected from an interval above 375.30 m can be used to analyze the relative changes of the SST.

5 Conclusions

(1) The paleo-SSTs reconstructed by the c(Mg)/c(Ca) ratios in the *A. radiata* skeletons from Well "Xike-1" reef core in the SCS show a general periodic trend of "high-low-high-low" in values changes since the Pliocene. The reconstructed paleo-SSTs fluctuated significantly, especially during the Quaternary, which overall showed a trend of rising. The changing process of the reconstructed paleo-SSTs can be substantially divided into four stages from the bottom to the upper: An interval of 0–63.30 m (about 0–0.8 Ma) corresponds to the fluctuating period of the reconstructed paleo-SSTs; an interval of 63.30–190.30 m (about 0.8–1.8 Ma) corresponds to a low temperature period; an interval of 190.30–2 246.30 m (about 1.8–2.7 Ma) corresponds to a high temperature period; whereas an interval of 246.30–375.30 m (about 2.7–5.3 Ma) corresponds to another low temperature period.

(2) The variations of c(Mg)/c(Ca) ratios in the *A. radiata* skeletons well recorded the major global paleoclimatic events. The fluctuating period of the reconstructed paleo-SSTs in an interval of 0–63.30 m corresponds to the four sub-glaciations of the Quaternary glaciation events. The low temperature period of the reconstructed paleo-SSTs in an interval of 246.30–272.30 m corres-

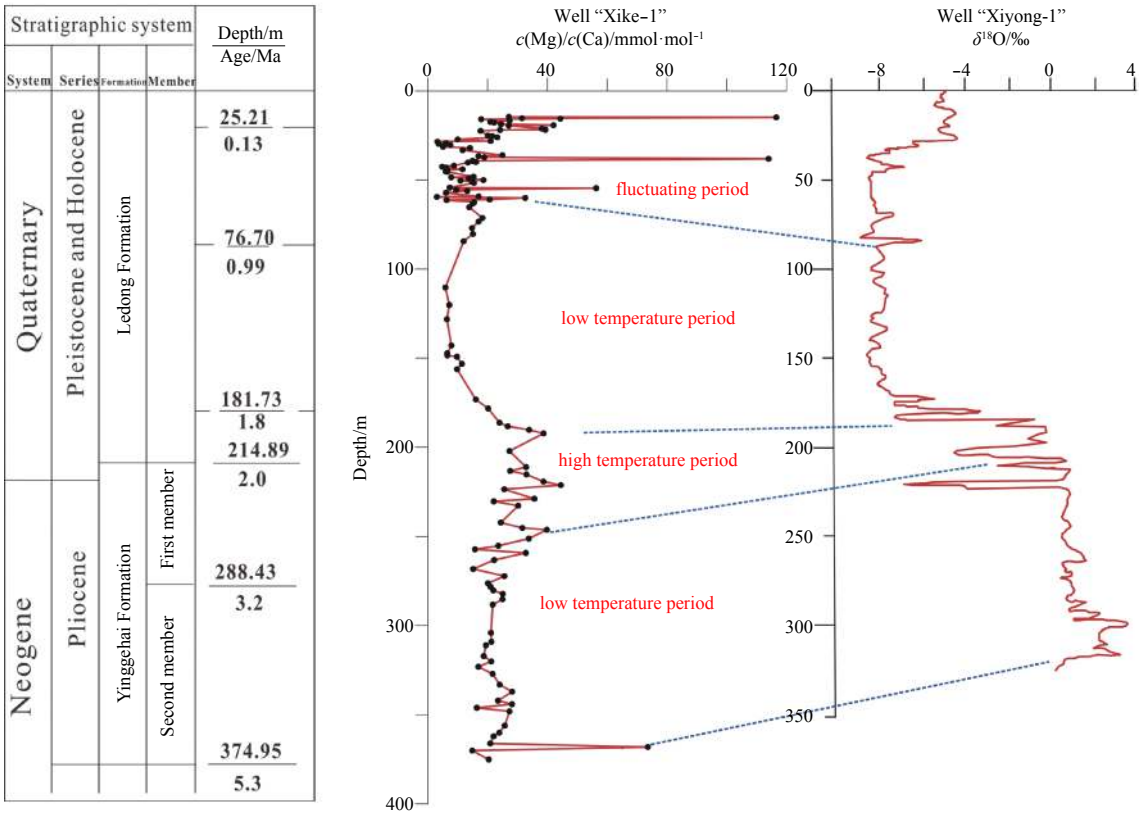

Fig. 10. Correspondence relationship between the changes of c(Mg)/c(Ca) ratios and that of the δ^{18}O values in the reef carbonates. The δ^{18}O data in the reef carbonates of Well "Xiyong-1" were derived from Zhao (2010).

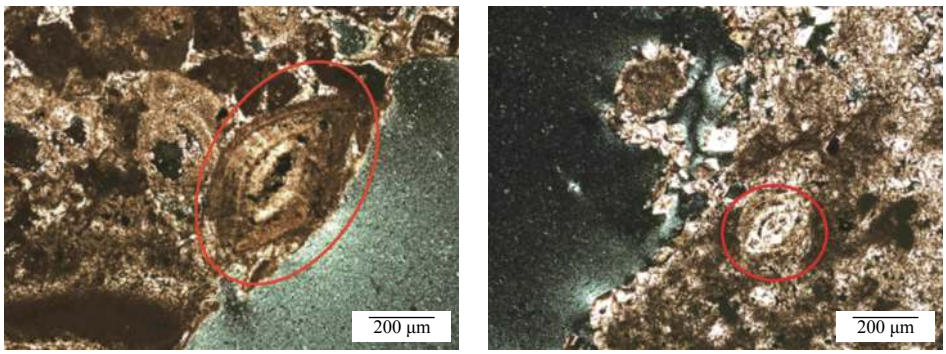

Fig. 11. Photomicrographs of *A. radiata* skeletons influenced by the diagenetic alteration. The sampling depth of the left one is 444.60 m. The sampling depth of the right one is 564.96 m.

ponds to the Arctic ice cap forming events during the Late Pliocene.

(3) The good corresponding relationship between the variations of c(Mg)/c(Ca) ratios in the *A. radiata* skeletons from Well "Xike-1" reef core and that of the δ^{18}O values in the carbonates of Well "Xiyong-1" reef core indicates that using the c(Mg)/c(Ca) ratios to reflect the relative changes of the SST is feasible and reliable in this area.

Acknowledgements

We thank Youhua Zhu from Chinese Academy of Sciences, Nanjing Institute of Geology and Palaeontology for her help in identifying the species of the foraminifera.

References

Barker S, Diz P, Vautravers M J, et al. 2009. Interhemispheric Atlantic seesaw response during the last deglaciation. Nature, 457(7233): 1097–1102, doi: 10.1038/nature07770

Bi Dongjie, Zhai Shikui, Zhang Daojun, et al. 2018. Constraints of fluid inclusions and C, O isotopic compositions on the origin of the dolomites in the Xisha Islands, South China Sea. Chemical Geology, 493: 504–517

Bi Dongjie, Zhang Daojun, Zhai Shikui, et al. 2017. The coupling relationships among the Qinghai-Tibet Plateau uplifting, the Qiongdongnan Basin subsiding and the Xisha Islands' reefs developing. Haiyang Xuebao (in Chinese), 39(1): 52–63

Bintanja R, Van De Wal R S W, Oerlemans J. 2005. Modelled atmospheric temperatures and global sea levels over the past million years. Nature, 437(7055): 125–128, doi: 10.1038/nature03975

Cao Jiaqi, Zhang Daojun, Zhai Shikui, et al. 2016. The characteristics and genetic model of the dolomitization in Xisha Reef Islands. Haiyang Xuebao (in Chinese), 38(11): 125–139

Deng Shoulin. 1992. Geographical Dictionary (in Chinese). Shijiazhuang: Hebei Education Press, 66–150

Ding Zhongli, Liu Dongsheng. 1991. Comparison of the paleoclimatic records in deep sea and loess since 1.8Ma. Chinese Science Bulletin (in Chinese), 36(18): 1401–1403

Elderfield H, Ferretti P, Greaves M, et al. 2012. Evolution of ocean temperature and ice volume through the Mid-Pleistocene climate transition. Science, 337(6095): 704–709, doi: 10.1126/science.1221294

Goldberg E D, Arrhenius G O S. 1958. Chemistry of pacific pelagic sediments. Geochimica et Cosmochimica Acta, 13(2–3): 153–212

Guo Qimei. 2013. Comparative analysis of sea surface temperature reconstruction methods. Acta Palaeontologica Sinica (in Chinese), 52(3): 399–406

Hasenfratz A P, Martínez-García A, Jaccard S L, et al. 2017. Determination of the Mg/Mn ratio in foraminiferal coatings: an approach to correct Mg/Ca temperatures for Mn-rich contaminant phases. Earth and Planetary Science Letters, 457: 335–347, doi: 10.1016/j.epsl.2016.10.004

He Qixiang, Zhang Mingshu, Han Chunrui. 1985. Ca, Mg, Sr geochemistry of recent carbonate sediments on Xisha Archipelago. Marine Geology and Quaternary Geology (in Chinese), 5(4): 31–40

Lea D W. 2003. Elemental and isotopic proxies of past ocean temperatures. Treatise on Geochemistry, 6: 1–26

Lea D W, Mashiotta T A, Spero H J. 1999. Controls on magnesium and strontium uptake in planktonic foraminifera determined by live culturing. Geochimica et Cosmochimica Acta, 63(16): 2369–2379, doi: 10.1016/S0016-7037(99)00197-0

Lea D W, Pak D K, Spero H J. 2000. Climate impact of late Quaternary equatorial Pacific sea surface temperature variations. Science, 289(5485): 1719–1724, doi: 10.1126/science.289.5485.1719

Li Siguang. 1940. The Quaternary glacier phenomenon in western Hubei, eastern Sichuan, western Hunan and northern Guizhou, China. Geological Review (in Chinese), (3): 171–184

Li Jianru. 2005. The application of foraminiferal shell Mg/Ca ratio in paleo-environmental studies. Advances in Earth Science (in Chinese), 20(8): 815–822

Li Qi, Li Qianyu, Wang Rujian. 2012. Progress in the paleoceanography of the South China Sea over the last 200 ka: a review. Advances in Earth Science (in Chinese), 27(2): 224–239

Li Xiaoyan, Shi Xuefa, Cheng Zhenbo, et al. 2008. Advances in study on the methods for sea surface paleotemperature reconstruction. Advances in Marine Science (in Chinese), 26(4): 512–521

Li Yue, Wang Rujian, Li Wenbao. 2016. Review on research on paleosea level reconstruction based on foraminiferal oxygen isotope in deep sea sediments. Advances in Earth Science (in Chinese), 31(3): 310–319

Liu Jianguo, Chen Muhong, Chen Zhong, et al. 2010. Clay mineral distribution in surface sediments of the South China Sea and its significance for in sediment sources and transport. Chinese Journal of Oceanology and Limnology, 28(2): 407–415, doi: 10.1007/s00343-010-9057-7

Ma Zhaoliang, Zhu Youhua, Liu Xinyu, et al. 2015. Quaternary calcareous algae from Well Xike-1 in Xisha Islands and its ecological function. Earth Science-Journal of China University of Geoscience (in Chinese), 40(4): 718–724, doi: 10.3799/dqkx.2015.059

Marshall J D, Ashton M. 1980. Isotopic and trace element evidence for submarine lithification of hardgrounds in the Jurassic of eastern England. Sedimentology, 27(3): 271–289, doi: 10.1111/sed.1980.27.issue-3

Marshall J F, McCulloch M T. 2002. An assessment of the Sr/Ca ratio

in shallow water hermatypic corals as a proxy for sea surface temperature. Geochimica et Cosmochimica Acta, 66(18): 3263–3280, doi: 10.1016/S0016-7037(02)00926-2

Nürnberg D. 1995. Magnesium in tests of *Neogloboquadrina pachyderma* sinistral from high northern and southern latitudes. Journal of Foraminiferal Research, 25(4): 350–368, doi: 10.2113/gsjfr.25.4.350

Nürnberg D, Bijma J, Hemleben C. 1996. Assessing the reliability of magnesium in foraminiferal calcite as a proxy for water mass temperatures. Geochimica et Cosmochimica Acta, 60(5): 803–814, doi: 10.1016/0016-7037(95)00446-7

Oppo D W, Sun Youbin. 2005. Amplitude and timing of sea-surface temperature change in the northern South China Sea: dynamic link to the East Asian monsoon. Geology, 33(10): 785–788, doi: 10.1130/G21867.1

Pelejero C, Grimalt J O, Heilig S, et al. 1999. High-resolution U_{37}^{K} temperature reconstructions in the South China Sea over the past 220 kyr. Paleoceanography, 14(2): 224–231, doi: 10.1029/1998PA900015

Prezbindowski D R. 1985. Burial cementation—is it important? A case study, Stuart City trend, south central Texas. AAPG Bulletin, 67: 241–245

Qiao Peijun, Zhu Weilin, Shao Lei, et al. 2015. Carbonate stable isotope stratigraphy of well XiKe-1, Xisha Islands. Earth Science-Journal of China University of Geoscience (in Chinese), 40(4): 725–732, doi: 10.3799/dqkx.2015.060

Raymo M E. 1997. The timing of major climate terminations. Paleoceanography, 12(4): 577–585, doi: 10.1029/97PA01169

Rosenthal Y, Boyle E A, Slowey N. 1997. Temperature control on the incorporation of magnesium, strontium, fluorine, and cadmium into benthic foraminiferal shells from Little Bahama Bank: Prospects for thermocline paleoceanography. Geochimica et Cosmochimica Acta, 61(17): 3633–3643, doi: 10.1016/S0016-7037(97)00181-6

Russell A D, Emerson S, Nelson B K, et al. 1994. Uranium in foraminiferal calcite as a recorder of seawater uranium concentrations. Geochimica et Cosmochimica Acta, 58(2): 671–681, doi: 10.1016/0016-7037(94)90497-9

Rutter N, Ding Zhongli, Evans M E, et al. 1990. Magnetostratigraphy of the Baoji loess-paleosol section in the north-central China Loess Plateau. Quaternary International, 7–8: 97–102

Sarnthein M, Pflaumann U, Wang Pinxian, et al. 1994. Preliminary report on Sonne-95 cruise monitor monsoon to the South China Sea. Reports, Geol-Palaont Inst Univ Kiel, 68: 5–39

Swart P K. 1981. The strontium, magnesium and sodium composition of recent scleractinian coral skeletons as standards for palaeoenvironmental analysis. Palaeogeography, Palaeoclimatology, Palaeoecology, 34: 115–136, doi: 10.1016/0031-0182(81)90060-2

Tamburini F, Adatte T, Föllmi K, et al. 2003. Investigating the history of East Asian monsoon and climate during the last glacial-interglacial period (0–140 000 years): mineralogy and geochemistry of ODP Sites 1143 and 1144, South China Sea. Marine Geology, 201(1–3): 147–168

Veizer J. 1989. Strontium isotopes in seawater through time. Annual Review of Earth and Planetary Sciences, 17(1): 141–167, doi: 10.1146/annurev.ea.17.050189.001041

Vollstaedt H, Eisenhauer A, Wallmann K, et al. 2014. The Phanerozoic $\delta^{88/86}$Sr record of seawater: New constraints on past changes in oceanic carbonate fluxes. Geochimica et Cosmochimica Acta, 128: 249–265, doi: 10.1016/j.gca.2013.10.006

Wang Guozhong. 2001. Sedimentology of the Coral Reefs in the South China Sea Area (in Chinese). Beijing: China Ocean Press, 1–313

Wang Zhenfeng, Cui Yuchi, Shao Lei, et al. 2015a. Carbonate platform development and sea-level variations of Xisha Islands: based on BIT index of Well Xike-1. Earth Science-Journal of China University of Geoscience (in Chinese), 44(5): 900–908

Wang Chongyou, He Xixian, Qiu Songyu. 1979. Preliminary study on the carbonate rocks and microfossils of the well "Xiyong-1", Xisha Islands. Petroleum Geology and Experiment (in Chinese), 1: 23–38

Wang L, Sarnthein M, Erlenkeuser H, et al. 1999. East Asian monsoon climate during the Late Pleistocene: high-resolution sediment records from the South China Sea. Marine Geology, 156(1–4): 245–284

Wang Xin, Shi Xuefa, Wang Guoqing, et al. 2015b. Late Quaternary sedimentary environmental evolution offshore of the Hangzhou Bay, East China-Implications for sea level change and formation of Changjiang alongshore current. Chinese Journal of Oceanology and Limnology, 33(3): 748–763, doi: 10.1007/s00343-015-4172-0

Wang Pinxian, Tian Jun, Cheng Xinrong. 2001. Transition of Quaternary glacial cyclicity in deep-sea records at Nansha, the South China Sea. Science in China Series: D Earth Sciences, 44(10): 926–933, doi: 10.1007/BF02907085

Wang Pinxian, Zhao Quanhong, Jian Zhimin, et al. 2003. Thirty million year deep sea records in the South China Sea. Chinese Science Bulletin, 48(23): 2524–2535, doi: 10.1007/BF03037016

Wei Gangjian, Li Xianhua, Nie Baofu, et al. 1999. High resolution porites Mg/Ca thermometer for the north of the South China Sea. Chinese Science Bulletin, 44(3): 273–276, doi: 10.1007/BF02896292

Wei Gangjian, Deng Wenfeng, Liu Ying, et al. 2007. High-resolution sea surface temperature records derived from foraminiferal Mg/Ca ratios during the last 260 ka in the northern South China Sea. Palaeogeography, Palaeoclimatology, Palaeoecology, 250(1-4): 126–138

Wei Gangjian, Sun Min, Li Xianhua, et al. 2000. Mg/Ca, Sr/Ca and U/Ca ratios of a porites coral from Sanya Bay, Hainan Island, South China Sea and their relationships to sea surface temperature. Palaeogeography, Palaeoclimatology, Palaeoecology, 162(1-2): 59–74

Xie Qiang, Wu Xiangyu, Yuan Wenya, et al. 2007. Life cycle of intraseasonal oscillation of summer SST in the western South China Sea. Acta Oceanologica Sinica, 26(3): 1–8

Xiu Chun, Luo Wei, Yang Hongjun, et al. 2015. Geochemical characteristics of reef carbonate Rocks in well Xike-1 of Shidao Island, Xisha area. Earth Science-Journal of China University of Geoscience (in Chinese), 40(4): 645–652, doi: 10.3799/dqkx.2015.051

Yang Zigeng, Li Youjun, Ding Qiuling, et al. 1979. Several problems of the Quaternary geology in eastern Hebei Plain. Acta Geologica Sinica (in Chinese), (4): 263–279

Yang Huairen, Xu Xin. 1980. Evolution of the Quaternary natural environment in eastern China. Journal of Nanjing University: Natural Sciences (in Chinese), (1): 121–144

You Li, Yu Yaping, Liao Jing, et al. 2015. Petrological charateristics and pore types of quaternary reef adjacent typical exposed surface in well Xike-1, Xisha Islands. Earth Science-Journal of China University of Geoscience (in Chinese), 40(4): 671–676, doi: 10.3799/dqkx.2015.054

Zhai Shikui, Mi Lijun, Shen Xing, et al. 2015. Mineral compositions and their environmental implications in reef of Shidao Island, Xisha. Earth Science-Journal of China University of Geoscience (in Chinese), 40(4): 597–605, doi: 10.3799/dqkx.2015.047

Zhang Daojun, Liu Xinyu, Wang Yahui, et al. 2015. Sedimentary evolution and reservoir characteristics of carbonate rocks since Late Miocene in Xisha area of the South China Sea. Earth Science-Journal of China University of Geoscience (in Chinese), 40(4): 606–614, doi: 10.3799/dqkx.2015.048

Zhang Mingshu, Liu Jian, Zhou Moqing. 1994. Study on magnetic susceptibility of the Well "Xiyong-1". Chinese Science Bulletin

(in Chinese), 39(4): 340–343

Zhang Haisheng, Zhou Huaiyang, Lu Bing, et al. 2005. Environmental change of palaeo-oceanography recorded in the sediment stratum in the northern part of South China Sea since the post glacial period. Haiyang Xuebao (in Chinese), 27(3): 52–58

Zhao Jingbo. 1985. Periglacial vegetation and quaternary glaciers. Geological Review (in Chinese), 31(6): 551–558

Zhao Jingbo. 1986. Vegetation type and climate during the Quaternary in the plain of North China. Scientia Geographica Sinica (in Chinese), 6(2): 151–157

Zhao Qiang. 2010. The sedimentary research about reef carbonatite in Xisha Islands waters [dissertation]. Qingdao: the Institute of Oceanology, the Chinese Academy of Sciences

Zhao Quanhong, Jian Zhimin, Wang Jiliang, et al. 2001. Neogene oxygen isotopic stratigraphy, ODP Site 1148, northern South China Sea. Science in China: Series D. Earth Sciences, 44(10): 934–942, doi: 10.1007/BF02907086

Zhao Quanhong, Wang Pinxian. 1999. Progress in quaternary paleoceanography of the South China Sea: a review. Quaternary Sciences (in Chinese), (6): 481–501

Zhao Qiang, Wu Shiguo, Xu Hong, et al. 2011. Sedimentary facies and evolution of aeolianites on Shidao Island, Xisha Islands. Chinese Journal of Oceanology and Limnology, 29(2): 398–413, doi: 10.1007/s00343-011-0018-6

Zhao Shuang, Zhang Daojun, Liu Li, et al. 2015. Diagenetic characteristics of Quaternary Reef-Carbonates from Well Xike-1, Xisha Islands, the South China Sea. Earth Science-Journal of China University of Geoscience (in Chinese), 44(5): 711–717

Zhu Weilin, Wang Zhenfeng, Mi Lijun, et al. 2015. Sequence stratigraphic framework and reef growth unit of Well Xike-1 from Xisha Islands, South China Sea. Earth Science-Journal of China University of Geoscience (in Chinese), 40(4): 677–687, doi: 10.3799/dqkx.2015.055